PROCEEDINGS OF SCIENCE

The Cosmic-ray Electron and Positron Spectrum Measured with MAGIC

Yating Chai,[a,*] Kazuma Ishio,[b] Daniel Kerszberg[c] and Salvatore Mangano[d] on behalf of the MAGIC collaboration

[a] *Max-Planck-Institut für Physik, Föhringer Ring 6, 80805, München, Germany*
[b] *Wydział Fizyki, Astronomii i Informatyki Stosowanej Institut Astronomii Uniwersytet Mikołaja Kopernika w Toruniu, Piwnice k. Torunia, 87-148 Łysomice, Poland*
[c] *Institut de Física d'Altes Energies, Edifici Cn, Campus UAB, 08193 Bellaterra (Barcelona), Spain*
[d] *Centro de Investigaciones Energéticas, Medioambientales y Tecnológicas Avda. Complutense, 40, 28.040. Madrid, Spain*

E-mail: ytchai@mpp.mpg.de

Cosmic-ray electrons and positrons (CREs) of TeV energies suffer severe energy loss during propagation due to inverse Compton scattering and synchrotron radiation process, they are therefore very useful to constrain the local cosmic-ray sources in the Galaxy. The ability to measure CREs by ground-based imaging atmospheric Cherenkov telescopes (IACTs) has been demonstrated in the past. In this proceeding, we will present two methods – a template fit method and a tight cut method based on a two-steps-trained Random Forest (RF) – optimized for the detection and study of CREs and will report on the measurement of the CREs energy spectrum from 300 GeV to 6 TeV with the MAGIC telescopes.

38th International Cosmic Ray Conference (ICRC2023)
26 July - 3 August, 2023
Nagoya, Japan

*Speaker

PoS(ICRC2023)323

1. Introduction

High-energy comsic-ray electrons and positrons (CREs) serve as a valuable tool for investigating local Galactic sources. This is because the limited travel distance of TeV CREs, restricted by energy loss through inverse Compton scattering and synchrotron radiation processes, prevents them from traveling beyond ~1 kiloparsec [1]. Potential astrophysical sources of CREs, such as nearby pulsars [2] and supernova remnants [3], have been proposed. In addition to the CRE spectrum, the positron fraction $f_{e^+}(E) = \Phi_{e^+}(E)/(\Phi_{e^+}(E) + \Phi_{e^-}(E))$, where Φ_{e^+} and Φ_{e^-} represent the fluxes of positrons and electrons respectively, is expected to conform to the "standard model". According to this model, the positron fraction decreases with energy, assuming that positrons originate from secondary production between cosmic rays and the interstellar medium.

Direct measurements of CREs have been conducted by PAMELA [4], AMS [5], and Fermi-LAT [6], providing large statistics for energies up to hundreds of GeV. However, for the TeV energy range, detectors with larger acceptance are required. Ground-based IACTs have proven to be capable of providing large statistics of CREs in the TeV range, with collection areas around 10^4 times greater than space-based instruments. The CRE spectrum exhibits a break at around 1 TeV, initially observed by H.E.S.S. [7], and later confirmed by direct measurements from DAMPE [9] and CALET [8]. As for the positron fraction spectrum, PAMELA [10] and AMS [11, 13] displays an unexpected upturn for energies above 10 GeV, suggesting the presence of additional sources beyond those predicted by the "standard model". Investigating the possible sources to explain the anomaly in the positron fraction spectrum has attracted significant attention, including astrophysical models and intriguing possibilities like dark matter particle annihilation or decay.

To solve the mystery of where TeV CREs come from and understand the unexpected increase in the positron fraction, it is important to have models that can explain both the CRE spectrum and the positron spectrum simultaneously. This makes it crucial to accurately measure CREs with large amounts of data using IACTs. These measurements will greatly contribute to our understanding of the origin of CREs and help narrow down the possible explanations.

2. Observation and Data

MAGIC is a stereoscopic system located at the El Roque de los Muchachos observatory in La Palma, Spain. It consists of two IACTs with a diameter of 17 meters each. The observatory is situated at coordinates 28.8°N, 17.8°W at an elevation of around 2200 meters.

IACTs detect the emission of Cherenkov light produced by charged particles of atmospheric showers, which are generated by the interaction of primary particles with the Earth's atmosphere. Therefore they cannot distinguish between CREs and γ-rays, since they call initiate electromagnetic showers. For this reason, the careful selection of the field of view (FoV) is crucial to minimize the contamination from γ-rays. The MAGIC data used in this analysis have been chosen based on the following criteria:

- Located at Galactic latitude $|b| > 20°$ to reduce the contamination from diffuse γ-ray emission from the Galactic plane.
- No known point γ-ray emission from the FoVs.

- No bright stars in the FoVs to reduce the noise caused by star light.

In this analysis, only events with a zenith distance below 35 degrees and observed under favorable weather conditions were selected. Approximately 220 hours of MAGIC data were used, and the low-level analysis was conducted using the standard software MARS [12] developed by MAGIC.

3. Methods

The primary challenge in CRE analysis lies in effectively rejecting background events. In the standard analysis of MAGIC, the background is estimated by considering the corresponding regions in the camera where no signal events are anticipated. However, due to the diffuse nature of CREs, the background estimation cannot be performed using the same approach. In this proceeding, two methods are introduced.

3.1 RF-Fit method

The RF-Fit method is a commonly used template fit method in previous CRE spectrum analyses with IACTs. This method involves employing templates for both the background and signal components in order to fit with real data. The background template is based on a large dataset of proton and helium Monte Carlo (MC) simulations, while the signal template consists of MC CREs. To distinguish between particle species, a machine learning technique called Random Forest (RF) is used to calculate a parameter known as "hadronness", which indicates the likelihood of a particle being classified as a hadron. In this analysis, diffuse MC protons and MC CREs are used as training samples to develop the hadronness estimator. This estimator is then applied to another samples of MC hadrons and MC CREs, as well as real data. Each event is assigned a hadronness value ranging from 0 to 1, where a value close to 0 suggests a high likelihood of being a signal event, while a background template is expected to have a higher hadronness value, i.e., closer to 1.

The distribution of hadronness is influenced by the distribution of pointing directions. To minimize the systematic uncertainties caused by the pointing directions, a tracking MC simulation method has been developed, allowing background and signal events to be simulated with the same pointing trajectories as the actual data. For the templates, events are selected if their incoming direction is within 1 degree around the camera center. The hadronness distribution of two templates, one for the hadronic background events and one for the signal events, are then fitted to the real data to determine the scaling factors. This is achieved through an extended likelihood fit within the hadronness range 0 to 0.4. An example of a template fit for the energy range between 598.6 GeV and 753.6 GeV is shown in Figure 1.

In each energy range, optimized hadronness cuts are implemented to achieve the highest significance. After applying the hadronness cut, the number of excess events is obtained using the equation $N_{\rm exc} = N_{\rm obs} - A \cdot N_{\rm had}$, where $N_{\rm obs}$ is the number of observed events, A is the scaling factor from the fit for the hadronic template, and $N_{\rm had}$ represents the number of events of hadronic template.

3.2 Two-Step RF method

The Two-Step RF method is a novel approach that uses the RF algorithm twice, where the second time of RF algorithm effectively distinguish signal events from signal-like background

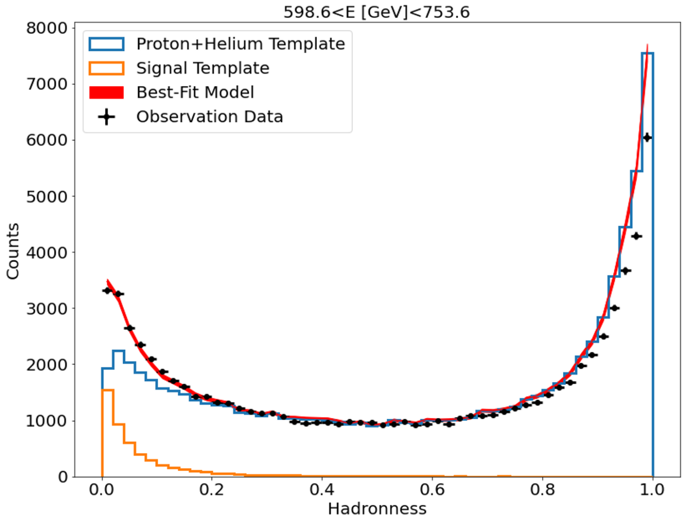

Figure 1: An example of a template fit is presented for the energy range spanning from 598.6 GeV to 753.6 GeV. The hadronness distributions of proton+helium and signal events are represented by blue and orange histograms, respectively. The red band represents the best fit model. Signal events tend to have hadronness values near 0, while hadronic events exhibit hadronness values closer to 1.

events. In first RF, all the MC protons and CREs are used to train the RF and generate the initial estimator. Second RF takes advantage of the hadronness information estimated by the first RF. Specifically, the second RF is trained using MC protons and CREs with a hadronness value lower than 0.3. This allows the new RF to discern subtle differences between the signal and signal-like hadronic events. Figure 2 illustrates the hadronness distribution of protons obtained through the First Step RF and the Second Step RF in the range 0 to 0.5. When hadronness is estimated using the First RF, the number of proton events steadily increases from 0 to 0.1 and then remains relatively constant from 0.1 to 0.5. On the other hand, when hadronness is estimated using the second RF, the number of proton events is significantly reduced in the low hadronness region.

The number of background events is significantly reduced in the low hadronness region when using the second RF for hadronness estimation. Consequently, after applying a very tight hadronness cut, only few background events are expected to remain. There is an example to show how the cut position for energy bin from 1194.3 GeV to 1503.6 GeV is determined based on the flux versus efficiency as depicted by the blue dots in the right panel of Figure 3.

Theoretically, as the hadronness efficiency increases, the flux gradually rises due to the increasing level of contamination. Some fluctuations are observed at very low hadronness efficiency levels, but they eventually stabilize. The fluctuations in the first few bins could be attributed to either insufficient statistics or discrepancies between the MC and observed data resulting from excessively low efficiency cuts. It is possible that both factors contribute to the observed fluctuations. The best-cut position, indicated by the red dot, is determined based on the minimum contamination after considering the fluctuations.

The expected contamination rates resulting from the survived efficiency cuts are estimated. The contamination from γ-rays is negligible thanks to the careful data selection process. Additionally, the contamination from helium is also negligible due to the high electron and hadron separation

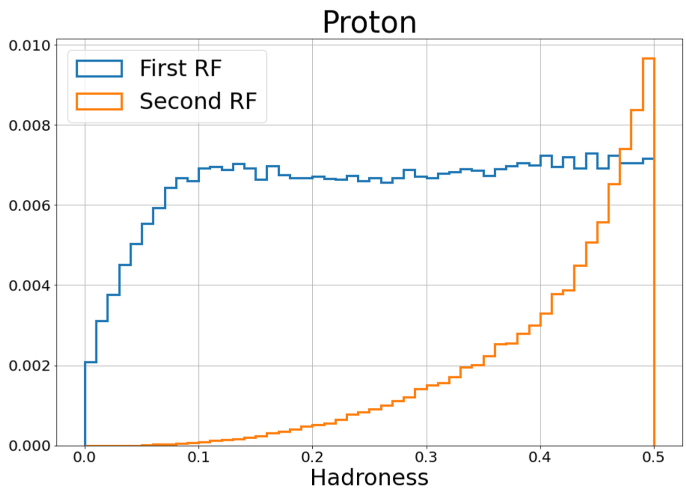

Figure 2: Comparison of the hadronness distribution of protons calculated by the First Step RF and the Second Step RF. It is observed that the number of proton events in the low hadronness region is considerably reduced when utilizing the Second Step RF. This reduction enables the application of a very stringent hadronness cut, resulting in a higher purity of signal events.

power of the second RF. Therefore only the contamination from protons are considered. The steps to calculate the contamination rates from protons are as follows:

- Calculate the flux ratio of protons to CREs using published data, which is approximately 530 at an energy of 400 GeV Using AMS resuls [5, 14].
- Determine the collection area ratio of protons and CREs based on the efficiency cuts. This is done by estimating the collection areas using MC simulations for protons and CREs.
- Use the flux ratio and collection area ratio to calculate the contamination rates from protons. The contamination rates can be seen in the left panel of Figure 3.

After subtracting the corresponding contamination rates at each efficiency position, the flux multiplied by E^3 without contamination is represented by the orange dots in the right panel of Figure 3. The orange dots, representing the the flux multiplied by E^3 without contamination, demonstrate a relatively stable pattern compared to the rising trend observed in the flux with contamination. However, there remains a systematic difference among the contamination-subtracted data points with different efficiencies, especially between the best-cut position and the efficiency cut by 10%.

4. Spectrum

Using the two methods, the energy spectrum of CREs was calculated across the energy range of 300 GeV to 6 TeV. Both methods yield consistent spectra, which can be described by a broken power-law function. The break energy is estimated to be around 900 GeV. Below the break energy, the energy index of the spectrum is approximately -3, while above the break energy, the index

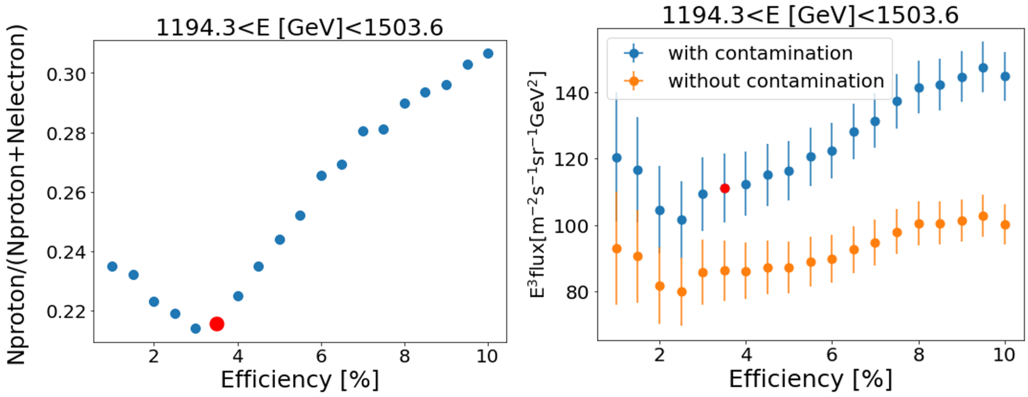

Figure 3: The left panel shows the contamination rates vary with changes in the hadronness efficiency at energy range from 1194.3 GeV to 1503.6 GeV. The best-cut position is shown as a red dot. The right panel shows the flux multiplied by E^3 after the subtraction of contamination.

is around -3.7. The goodness-of-fit statistics, represented by χ^2/dof, are 2.44/6 for the RF-Fit method and 1.56/4 for the Two-Step RF method. The main source of systematic uncertainty arises from the energy reconstruction, with an estimated uncertainty of 15%.

References

[1] Aharonian, F. A. and Atoyan, A. M. and Volk, H. J., High energy electrons and positrons in cosmic rays as an indicator of the existence of a nearby cosmic tevatron, Astron. Astrophys., 294, L41–L44, 1995

[2] Tim Linden and Stefano Profumo, Probing the Pulsar Origin of the Anomalous Positron Fraction with AMS-02 and Atmospheric Cherenkov Telescopes, 772(01):18, 2013

[3] M. Di Mauro and F. Donato and N. Fornengo and R. Lineros and A. Vittino, Interpretation of AMS-02 electrons and positrons data, Journal of Cosmology and Astroparticle Physics, 2014 (04):006–006, 2014

[4] Adriani, O. et al. Cosmic-Ray Electron Flux Measured by the PAMELA Experiment between 1 and 625 GeV, 106, 201101, 2011

[5] Aguilar, M. et al. Electron and Positron Fluxes in Primary Cosmic Rays Measured with the Alpha Magnetic Spectrometer on the International Space Station, Phys. Rev. Lett., 113, 121102, 2014

[6] Abdollahi, S. et al., Cosmic-ray electron-positron spectrum from 7 GeV to 2 TeV with the Fermi Large Area Telescope, Physical Review D, 95, 8, 2017

[7] Aharonian, F. et al., Energy Spectrum of Cosmic-Ray Electrons at TeV Energies, Physical Review Letters, 101, 261104, 2008

PoS(ICRC2023)323

[8] Adriani, O. et al. Extended Measurement of the Cosmic-Ray Electron and Positron Spectrum from 11 GeV to 4.8 TeV with the Calorimetric Electron Telescope on the International Space Station, 120, 261102, 2018

[9] Ambrosi, G. et al. Direct detection of a break in the teraelectronvolt cosmic-ray spectrum of electrons and positrons, Naure, 552, 63–66, 2017

[10] Adriani, O. et al., An anomalous positron abundance in cosmic rays with energies 1.5 –100 GeV, Nature, 458(7238):607–609, 2009

[11] Aguilar, M. et al. First Result from the Alpha Magnetic Spectrometer on the International Space Station: Precision Measurement of the Positron Fraction in Primary Cosmic Rays of 0.5–350 GeV, Phys. Rev. Lett., 110, 141102, 2013

[12] A. Moralejo et al., MARS, the MAGIC Analysis and Reconstruction Software, 0907.0943, 2009

[13] Accardo, L. et al. High Statistics Measurement of the Positron Fraction in Primary Cosmic Rays of 0.5–500 GeV with the Alpha Magnetic Spectrometer on the International Space Station, Phys. Rev. Lett., 113, 121101, 2014

[14] Zhao, F. et al., Improvement of cosmic-ray proton measurement with the electromagnetic calorimeter of the Alpha Magnetic Spectrometer, Radiation Detection Technology and Methods, 5, 90–94, 2021

PoS(ICRC2023)323

Full Authors List: MAGIC Collaboration

H. Abe[1], S. Abe[1], J. Abhir[2], V. A. Acciari[3], I. Agudo[4], T. Aniello[5], S. Ansoldi[6,46], L. A. Antonelli[5], A. Arbet Engels[7], C. Arcaro[8], M. Artero[9], K. Asano[1], D. Baack[10], A. Babić[11], A. Baquero[12], U. Barres de Almeida[13], J. A. Barrio[12], I. Batković[8], J. Baxter[1], J. Becerra González[3], W. Bednarek[14], E. Bernardini[8], M. Bernardos[4], J. Bernete[15], A. Berti[7], J. Besenrieder[7], C. Bigongiari[5], A. Biland[2], O. Blanch[9], G. Bonnoli[5], Ž. Bošnjak[11], I. Burelli[6], G. Busetto[8], A. Campoy-Ordaz[16], A. Carosi[5], R. Carosi[17], M. Carretero-Castrillo[18], A. J. Castro-Tirado[4], G. Ceribella[7], Y. Chai[7], A. Chilingarian[19], A. Cifuentes[15], S. Cikota[11], E. Colombo[3], J. L. Contreras[12], J. Cortina[15], S. Covino[5], G. D'Amico[20], V. D'Elia[5], P. Da Vela[17,47], F. Dazzi[5], A. De Angelis[8], B. De Lotto[6], A. Del Popolo[21], M. Delfino[9,48], J. Delgado[9,48], C. Delgado Mendez[15], D. Depaoli[22], F. Di Pierro[22], L. Di Venere[23], D. Dominis Prester[24], A. Donini[5], D. Dorner[25], M. Doro[8], D. Elsaesser[10], G. Emery[26], J. Escudero[4], L. Fariña[9], A. Fattorini[10], L. Foffano[5], L. Font[16], S. Fröse[10], S. Fukami[2], Y. Fukazawa[27], R. J. García López[3], M. Garczarczyk[28], S. Gasparyan[29], M. Gaug[16], J. G. Giesbrecht Paiva[13], N. Giglietto[23], F. Giordano[23], P. Gliwny[14], N. Godinović[30], R. Grau[9], D. Green[7], J. G. Green[7], D. Hadasch[1], A. Hahn[7], T. Hassan[15], L. Heckmann[7,49], J. Herrera[3], D. Hrupec[31], M. Hütten[1], R. Imazawa[27], T. Inada[1], R. Iotov[25], K. Ishio[14], I. Jiménez Martínez[15], J. Jormanainen[32], D. Kerszberg[9], G. W. Kluge[20,50], Y. Kobayashi[1], P. M. Kouch[32], H. Kubo[1], J. Kushida[33], M. Láinez Lezáun[12], A. Lamastra[5], D. Lelas[30], F. Leone[5], E. Lindfors[32], L. Linhoff[10], S. Lombardi[5], F. Longo[6,51], R. López-Coto[4], M. López-Moya[12], A. López-Oramas[3], S. Loporchio[23], A. Lorini[34], E. Lyard[26], B. Machado de Oliveira Fraga[13], P. Majumdar[35], M. Makariev[36], G. Maneva[36], N. Mang[10], M. Manganaro[24], S. Mangano[15], K. Mannheim[25], M. Mariotti[8], M. Martínez[9], M. Martínez-Chicharro[15], A. Mas-Aguilar[12], D. Mazin[1,52], S. Menchiari[34], S. Mender[10], S. Mićanović[24], D. Miceli[8], T. Miener[12], J. M. Miranda[34], R. Mirzoyan[7], M. Molero González[3], E. Molina[3], H. A. Mondal[35], A. Moralejo[9], D. Morcuende[12], T. Nakamori[37], C. Nanci[5], L. Nava[5], V. Neustroev[38], L. Nickel[10], M. Nievas Rosillo[3], C. Nigro[9], L. Nikolić[34], K. Nilsson[32], K. Nishijima[33], T. Njoh Ekoume[3], K. Noda[39], S. Nozaki[7], Y. Ohtani[1], T. Oka[40], A. Okumura[41], J. Otero-Santos[3], S. Paiano[5], M. Palatiello[6], D. Paneque[7], R. Paoletti[34], J. M. Paredes[18], L. Pavletić[24], D. Pavlović[24], M. Persic[6,53], M. Pihet[8], G. Pirola[7], F. Podobnik[34], P. G. Prada Moroni[17], E. Prandini[8], G. Principe[6], C. Priyadarshi[9], W. Rhode[10], M. Ribó[18], J. Rico[9], C. Righi[5], N. Sahakyan[29], T. Saito[1], S. Sakurai[1], K. Satalecka[32], F. G. Saturni[5], B. Schleicher[25], K. Schmidt[10], F. Schmuckermaier[7], J. L. Schubert[10], T. Schweizer[7], A. Sciaccaluga[5], J. Sitarek[14], V. Sliusar[26], D. Sobczynska[14], A. Spolon[8], A. Stamerra[5], J. Strišković[31], D. Strom[7], M. Strzys[1], Y. Suda[27], T. Surić[42], S. Suutarinen[32], H. Tajima[41], M. Takahashi[41], R. Takeishi[1], F. Tavecchio[5], P. Temnikov[36], K. Terauchi[40], T. Terzić[24], M. Teshima[7,54], L. Tosti[43], S. Truzzi[34], A. Tutone[5], S. Ubach[16], J. van Scherpenberg[7], M. Vazquez Acosta[3], S. Ventura[34], V. Verguilov[36], I. Viale[8], C. F. Vigorito[22], V. Vitale[44], I. Vovk[1], R. Walter[26], M. Will[7], C. Wunderlich[34], T. Yamamoto[45], [1] Japanese MAGIC Group: Institute for Cosmic Ray Research (ICRR), The University of Tokyo, Kashiwa, 277-8582 Chiba, Japan

[2] ETH Zürich, CH-8093 Zürich, Switzerland

[3] Instituto de Astrofísica de Canarias and Dpto. de Astrofísica, Universidad de La Laguna, E-38200, La Laguna, Tenerife, Spain

[4] Instituto de Astrofísica de Andalucía-CSIC, Glorieta de la Astronomía s/n, 18008, Granada, Spain

[5] National Institute for Astrophysics (INAF), I-00136 Rome, Italy

[6] Università di Udine and INFN Trieste, I-33100 Udine, Italy

[7] Max-Planck-Institut für Physik, D-80805 München, Germany

[8] Università di Padova and INFN, I-35131 Padova, Italy

[9] Institut de Física d'Altes Energies (IFAE), The Barcelona Institute of Science and Technology (BIST), E-08193 Bellaterra (Barcelona), Spain

[10] Technische Universität Dortmund, D-44221 Dortmund, Germany

[11] Croatian MAGIC Group: University of Zagreb, Faculty of Electrical Engineering and Computing (FER), 10000 Zagreb, Croatia

[12] IPARCOS Institute and EMFTEL Department, Universidad Complutense de Madrid, E-28040 Madrid, Spain

[13] Centro Brasileiro de Pesquisas Físicas (CBPF), 22290-180 URCA, Rio de Janeiro (RJ), Brazil

[14] University of Lodz, Faculty of Physics and Applied Informatics, Department of Astrophysics, 90-236 Lodz, Poland

[15] Centro de Investigaciones Energéticas, Medioambientales y Tecnológicas, E-28040 Madrid, Spain

[16] Departament de Física, and CERES-IEEC, Universitat Autònoma de Barcelona, E-08193 Bellaterra, Spain

[17] Università di Pisa and INFN Pisa, I-56126 Pisa, Italy

[18] Universitat de Barcelona, ICCUB, IEEC-UB, E-08028 Barcelona, Spain

[19] Armenian MAGIC Group: A. Alikhanyan National Science Laboratory, 0036 Yerevan, Armenia

[20] Department for Physics and Technology, University of Bergen, Norway

[21] INFN MAGIC Group: INFN Sezione di Catania and Dipartimento di Fisica e Astronomia, University of Catania, I-95123 Catania, Italy

[22] INFN MAGIC Group: INFN Sezione di Torino and Università degli Studi di Torino, I-10125 Torino, Italy

[23] INFN MAGIC Group: INFN Sezione di Bari and Dipartimento Interateneo di Fisica dell'Università e del Politecnico di Bari, I-70125 Bari, Italy

[24] Croatian MAGIC Group: University of Rijeka, Faculty of Physics, 51000 Rijeka, Croatia

[25] Universität Würzburg, D-97074 Würzburg, Germany

[26] University of Geneva, Chemin d'Ecogia 16, CH-1290 Versoix, Switzerland

[27] Japanese MAGIC Group: Physics Program, Graduate School of Advanced Science and Engineering, Hiroshima University, 739-8526 Hiroshima, Japan

[28] Deutsches Elektronen-Synchrotron (DESY), D-15738 Zeuthen, Germany

[29] Armenian MAGIC Group: ICRANet-Armenia, 0019 Yerevan, Armenia

PoS(ICRC2023)323

[30] Croatian MAGIC Group: University of Split, Faculty of Electrical Engineering, Mechanical Engineering and Naval Architecture (FESB), 21000 Split, Croatia
[31] Croatian MAGIC Group: Josip Juraj Strossmayer University of Osijek, Department of Physics, 31000 Osijek, Croatia
[32] Finnish MAGIC Group: Finnish Centre for Astronomy with ESO, University of Turku, FI-20014 Turku, Finland
[33] Japanese MAGIC Group: Department of Physics, Tokai University, Hiratsuka, 259-1292 Kanagawa, Japan
[34] Università di Siena and INFN Pisa, I-53100 Siena, Italy
[35] Saha Institute of Nuclear Physics, A CI of Homi Bhabha National Institute, Kolkata 700064, West Bengal, India
[36] Inst. for Nucl. Research and Nucl. Energy, Bulgarian Academy of Sciences, BG-1784 Sofia, Bulgaria
[37] Japanese MAGIC Group: Department of Physics, Yamagata University, Yamagata 990-8560, Japan
[38] Finnish MAGIC Group: Space Physics and Astronomy Research Unit, University of Oulu, FI-90014 Oulu, Finland
[39] Japanese MAGIC Group: Chiba University, ICEHAP, 263-8522 Chiba, Japan
[40] Japanese MAGIC Group: Department of Physics, Kyoto University, 606-8502 Kyoto, Japan
[41] Japanese MAGIC Group: Institute for Space-Earth Environmental Research and Kobayashi-Maskawa Institute for the Origin of Particles and the Universe, Nagoya University, 464-6801 Nagoya, Japan
[42] Croatian MAGIC Group: Ruđer Bošković Institute, 10000 Zagreb, Croatia
[43] INFN MAGIC Group: INFN Sezione di Perugia, I-06123 Perugia, Italy
[44] INFN MAGIC Group: INFN Roma Tor Vergata, I-00133 Roma, Italy
[45] Japanese MAGIC Group: Department of Physics, Konan University, Kobe, Hyogo 658-8501, Japan
[46] also at International Center for Relativistic Astrophysics (ICRA), Rome, Italy
[47] now at Institute for Astro- and Particle Physics, University of Innsbruck, A-6020 Innsbruck, Austria
[48] also at Port d'Informació Científica (PIC), E-08193 Bellaterra (Barcelona), Spain
[49] also at Institute for Astro- and Particle Physics, University of Innsbruck, A-6020 Innsbruck, Austria
[50] also at Department of Physics, University of Oslo, Norway
[51] also at Dipartimento di Fisica, Università di Trieste, I-34127 Trieste, Italy
[52] Max-Planck-Institut für Physik, D-80805 München, Germany
[53] also at INAF Padova
[54] Japanese MAGIC Group: Institute for Cosmic Ray Research (ICRR), The University of Tokyo, Kashiwa, 277-8582 Chiba, Japan

PoS(ICRC2023)323